Proceedings of Meetings on Acoustics

ECUA 2012 11th European Conference on Underwater Acoustics
Edinburgh, Scotland
2 - 6 July 2012
Session UW: Underwater Acoustics

UW170. Vector sensor geoacoustic estimation with standard arrays

Orlando Rodríguez*, Paulo Felisberto, Emanuel Ey, Joseph Schneiderwind and S. M. Jesus

*Corresponding author's address: Laboratório de Robótica e Sistemas em Engenharia e Ciência (LARSyS), Campus de Gambelas, Universidade do Algarve, Faro, 8005-139, N/A, Portugal, orodrig@ualg.pt

Vector Sensor Arrays (hereafter VSAs) are progressively becoming more and more attractive among the underwater acoustics community due to the advantages of VSAs over standard arrays of acoustic hydrophones. While the later record only acoustic pressure, VSAs record also particle velocity; such technical feature increases by a factor of four the amount of information that can be used for the processing ofacoustic data, leading to a substantial increase in performance. Since VSA sensor technology is relatively recent, and thus not yet fully available, one can consider the usage of closely located pairs of standard hydrophones, which can be used to estimate the vertical component of particle velocity as a difference of acoustic pressure, measured at each pair of hydrophones. The present discussion introduces a theoretical review of particle velocity calculations using different acoustic models, and tests the performance of estimators for geoacoustic inversion using acoustic pressure, particle velocity components and direct and approximated values of the vertical component only.

Published by the Acoustical Society of America through the American Institute of Physics

1 INTRODUCTION

Vector Sensor Arrays (hereafter VSAs) are progressively becoming more and more attractive among the underwater acoustics community, mainly due to the advantages of VSAs over arrays of standard hydrophones. While the later measure only acoustic pressure, VSAs measure particle velocity as well; such feature increases by a factor of four the amount of information that can be used for the processing of acoustic data, leading to a substantial improvement of array performance. Since VSA sensor technology is relatively recent, and thus not yet fully available, one can consider using closely located pairs of standard hydrophones to estimate the vertical component of particle velocity; the estimation uses the difference of acoustic pressure, measured at each pair. The present discussion introduces a review of particle velocity calculations based on the theoretical background provided by different acoustic models; additionally, the discussion tests the performance of geoacoustic estimation using acoustic pressure, particle velocity components, and direct and approximated values of the vertical component only. The conclusions are presented at the end of the discussion.

2 PARTICLE VELOCITY ESTIMATION

Particle velocity $\mathbf{v}$ is related to acoustic pressure P in the frequency domain through the relationship [1]

$$\mathbf{v} = -\frac{i}{\omega\rho}\nabla P \,, \tag{1}$$

where ρ represents the watercolumn density, and ω stands for the frequency of the propagating wave. The factors ρ and ω only affect the amplitude of particle velocity, while the imaginary unit implies a phase shift of $\pi/2$ radians. Without such factors particle velocity can be viewed as the gradient of acoustic pressure; therefore, the gradient of acoustic pressure will be identified as the particle velocity in the discussion that follows.

2.1 NORMAL MODE APPROACH

The typical normal mode approach is based on the solution of the wave equation for a waveguide with cylindrical symmetry, and further representation of acoustic pressure as the product of two functions; the first function is range dependent, while the second function is depth dependent. The differential equation for the depth dependent function provides a set of orthogonal solutions, called normal modes. The analytical expression for the normal mode expansion can then be written as [2]

$$P(r, z) = S(\omega)\frac{e^{i\pi/4}}{\rho(z_s)\sqrt{8\pi}}\sum_{m=1}^{M}u_m(z_s)\frac{e^{ik_m r}}{\sqrt{k_m r}}\,u_m(z) \tag{2}$$

where $S(\omega)$ stands for the source spectrum, z_s is the source depth and ρ stands for water density. It follows from Eq.(2) that the horizontal derivative of acoustic pressure corresponds, approximately, to

$$u \approx iS(\omega) \frac{e^{i\pi/4}}{\rho(z_s)\sqrt{8\pi}} \sum_{m=1}^{M} u_m(z_s) k_m \frac{e^{ik_m r}}{\sqrt{k_m r}} \, u_m(z) \tag{3}$$

while the vertical derivative corresponds (exactly) to:

$$w = S(\omega) \frac{e^{i\pi/4}}{\rho(z_s)\sqrt{8\pi}} \sum_{m=1}^{M} u_m(z_s) \frac{e^{ik_m r}}{\sqrt{k_m r}} \frac{du_m}{dz} \; . \tag{4}$$

Following [3] one can notice that both p and u are expanded on the basis of modes $u_m(z)$, while w is expanded on the basis of du_m/dz. In a general sense one can write that

$$\frac{du_m}{dz} \approx i\gamma_m u_m(z) \quad \text{where} \quad \gamma_m = \sqrt{\omega^2/c^2 - k_m^2} \quad \text{stands for the vertical wavenumber.} \tag{5}$$

Additionally, since γ_m increases with increasing mode number the net effect of the derivative is to enhance the contribution of higher modes in the field of w, relative to the stronger weighting of low order modes in the fields of p and u. Thus, Eq.(2) provides a clear framework to distinguish the different enhancement of modes in the fields of u and w. Additional approaches for the calculation of particle velocity from acoustic pressure will follow in the next sections. To this end and without loss of generality it will be considered that $S(\omega) = 1$ and $\rho(z) = $ constant.

2.2 GAUSSIAN BEAM APPROACH

Within the Gaussian beam approach the influence of a given ray to the field of acoustic pressure can be written as [4]

$$P(s,n) = \frac{1}{4\pi} \sqrt{\frac{c(s)}{c(0)} \frac{\cos\theta(0)}{q_\perp(s)q(s)}} \times \exp\left[-i\omega \left(\tau(s) + \frac{1}{2}\frac{p(s)}{q(s)}n^2 \right) \right] , \tag{6}$$

where s and n stand for the ray arclength and the ray normal, respectively, $c(s)$ stands for sound speed along the ray trajectory, $\theta(0)$ is the launching angle, and p and q are beam parameters, obtained from the solution of dynamic equations. The acoustic pressure at a given point is obtained summing the influences of different rays passing near the hydrophone. The pressure gradient can be written in terms of ray arclength and ray normal as

$$\nabla P = \frac{\partial P}{\partial n}\mathbf{e}_n + \frac{\partial P}{\partial s}\mathbf{e}_s , \tag{7}$$

where $\mathbf{e}_s$ and $\mathbf{e}_n$ are unitary vectors, oriented along s and n, respectively. The two vectors are related to the ray elevation θ through the relationships

$$\mathbf{e}_s = [\cos\theta, \sin\theta] \quad \text{and} \quad \mathbf{e}_n = [-\sin\theta, \cos\theta] \tag{8}$$

(see Fig.2.2). In order to obtain analytical expressions for the derivatives along n and s let us rewrite Eq.(6) as

$$P(s,n) = P_0(s) \exp\left[-i\omega \left(\frac{s}{c(s)} + \frac{1}{2}\gamma(s)n^2 \right) \right] , \tag{9}$$

where $s/c(s) = \tau(s)$ and $\gamma(s) = p(s)/q(s)$. Therefore, the first derivative corresponds exactly to

$$\frac{\partial P}{\partial n} = -i\omega\gamma(s)nP \; . \tag{10}$$

The exact derivative along s produces a cumbersome expression due to the dependence of the different factors on s. Since the exponential factor has the largest impact on the derivative one can write approximately that

$$\frac{\partial P}{\partial s} = -i\frac{\omega}{c(s)}P \; . \tag{11}$$

Further, the velocity components (u, w) can be calculated projecting the gradient components $\partial P / \partial n$ and $\partial P / \partial s$ onto the (r, z) axes as

$$u = (\nabla P \cdot \mathbf{e}_r) = -\frac{\partial P}{\partial n} \sin \theta + \frac{\partial P}{\partial s} \cos \theta \qquad (12)$$

and

$$w = (\nabla P \cdot \mathbf{e}_z) = \frac{\partial P}{\partial n} \cos \theta + \frac{\partial P}{\partial s} \sin \theta \qquad (13)$$

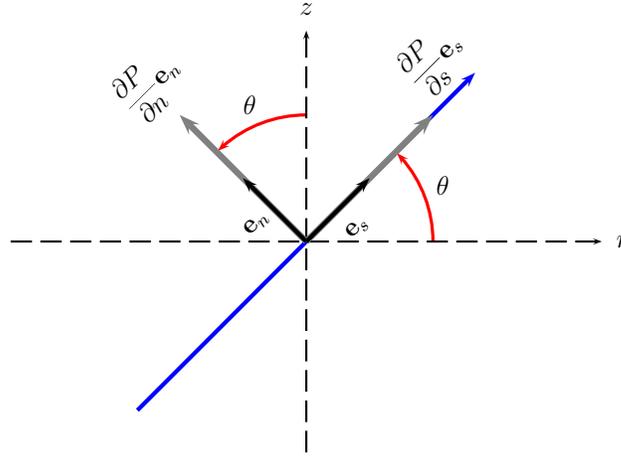where $\mathbf{e}_r$ and $\mathbf{e}_z$ stand for the unitary vectors along r and z, respectively.

Figure 1: Ray polarization vectors $\mathbf{e}_s$ and $\mathbf{e}_n$ and pressure gradient components along the n and s directions; θ stands for the ray elevation (i.e. the ray angle relative to the r axis).

2.3 PARABOLIC EQUATION APPROACH

The parabolic approach is based on the substitution of the wave equation with a parabolic equation (hereafter PE), which contains a single derivative along range; following [5, 6] one can write that

$$P(r, z) = P_0 \frac{1}{\sqrt{r}} \Psi(r, z) \exp(ik_0 r) \qquad (14)$$

where

$$\frac{\partial \Psi}{\partial r} = -ik_0 \hat{H} \Psi \ , \qquad (15)$$

$k_0 = \omega / c_0$, c_0 is a reference sound speed and $\hat{H}$ represents a total energy-like differential operator. Given $\Psi(0, z)$ a marching solution can be obtained by integrating Eq.(15) progressively along range through a split-step technique. PE models can be divided into two categories depending on how $\hat{H}$ is approximated, namely Padé approximations and spectral techniques. Padé approximations replace $\hat{H}$ with rational polynomials, which reduce Eq.(15) to a set of tridiagonal linear equations, which are solved at each range step. Spectral techniques rely on the properties of Fourier transforms to solve Eq.(15) in the wavenumber domain, providing the following marching solution [5]

$$\Psi(r + \Delta r, z) = \exp\left(-ik_0 \Delta r \hat{U}\right) \times \mathsf{FFT}\left[\exp\left(-ik_0 \Delta r \hat{T}\right) \times \hat{\Psi}(r, k)\right] \qquad (16)$$

where $\hat{\Psi}(r, k)$ is the inverse Fourier transform of $\Psi(r, z)$ and $\hat{T} + \hat{U} = \hat{H}$. The spectral technique allows to obtain closed-form analytical expressions for particle velocity; in particular (and without loss of generality) the operators $\hat{T}$ and $\hat{U}$ for the standard parabolic equation correspond to

$$\hat{T} = -\frac{1}{2k_0^2} \frac{\partial^2}{\partial z^2} \quad \text{and} \quad \hat{U} = -\frac{1}{2}\left(n^2 - 1\right) \ ,$$

where $n = c/c_0$. The corresponding expressions for u and w become

$$u = u_0 \exp\left(ik_0 r\right) \times \left(u_1 + u_2 - u_3\right) \ , \tag{17}$$

$$w = w_0 \exp\left(ik_0 r\right) \times \mathsf{FFT}\left[ik\hat{\Psi}(r,k)\right] \ , \tag{18}$$

where

$$u_1 = i\frac{\Psi(r,z)}{2k_0 r} \quad , \quad u_2 = \frac{1}{2}(n^2+1)\Psi(r,z)$$

and

$$u_3 = \mathsf{FFT}\left[\frac{1}{2}\left(\frac{k}{k_0}\right)^2 \hat{\Psi}(r,k)\right] \ .$$

2.4 INTERPOLATION (MODEL-INDEPENDENT) APPROACH

The previous approaches are all model-based in the sense that the calculation of u and w is based on derivatives of an analytical expression for acoustic pressure; such expressions are specific to the model considered. The approach used in the acoustic model TRACEO relies on a barycentric parabolic interpolator, which is used to estimate both horizontal and vertical derivatives. The interpolator is constructed using a star-like stencil of five points; the center of the star coincides with the position of the hydrophone, while the horizontal and vertical points are located at the left and right sides of the hydrophone, and also above and below it. Acoustic pressure is calculated at the five points of the stencil; the points aligned along the horizontal are used to calculate the horizontal derivative at the star's center; the vertical derivative at the same position is calculated using the points aligned along the vertical. The spacing between an outer point and the star's center corresponds to $\lambda/10$; such choice is expected to avoid frequency aliasing. The interpolator itself can be described as follows: let us consider a set of three points x_1, x_2 and x_3, and the corresponding function values $f(x_1)$, $f(x_2)$ and $f(x_3)$.
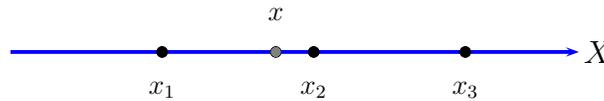

Figure 2: Barycentric parabolic interpolation.

At a given point x (see Fig.2) the interpolant can be written as

$$f(x) = f(x_1) + a_2\left(x-x_1\right)\left(x-x_3\right) + a_3\left(x-x_1\right)\left(x-x_2\right) \ . \tag{19}$$

It follows from this expression that

$$a_2 = \frac{f(x_2) - f(x_1)}{(x_2-x_1)(x_2-x_3)} \quad \text{and} \quad a_3 = \frac{f(x_3) - f(x_1)}{(x_3-x_1)(x_3-x_2)} \ .$$

The approximations to the derivatives become

$$\frac{df}{dx} = a_2\left(2x - x_1 - x_3\right) + a_3\left(2x - x_1 - x_2\right)$$

and

$$\frac{d^2 f}{dx^2} = 2\left(a_2 + a_3\right) \ .$$

The validity of the interpolation approach will be discussed in the following section.

3 TRACEO'S DESCRIPTION AND PRELIMINARY VALIDATION

TRACEO is a Gaussian beam model, which is under current development at the SiPLAB of the University of Algarve.[1] The model was developed in order to:

- Predict acoustic pressure and particle velocity in environments with elaborate upper and lower boundaries, which can be characterized by range-dependent compressional and shear properties. Modeling particle velocity is important for vector sensor applications and can be used, in particular, for geoacoustic inversion with high frequency data [7–9].

- Include one or more targets in the waveguide.

- Produce ray, eigenray, amplitude and travel time information. In particular, eigenrays are to be calculated even if rays are reflected backwards on targets located beyond the current position of the hydrophone.

A preliminary validation of TRACEO's accuracy for particle velocity calculations is presented here through the comparison between TRACEO's predictions and the exact results of particle velocity calculations for a Pekeris waveguide (shear included); the compressional and shear potentials of such a waveguide are well know in the literature, [10] and the particle velocity components are easily calculated from the analytic expressions for both potentials. The comparison is shown in Fig. 3 for the set of parameters f = 200 Hz, z_s = 69.1 m, z_r = 137.1 m, D = 145 m, c_p = 2290 m/s, c_s = 1050 m/s, ρ_b = 1.378 g/cm^3, α_p = 0.76 dB/λ and α_s = 1.05 dB/λ; in both cases the analytic solution is indicated by a solid curve, while TRACEO's prediction is indicated by a dashed curve. The interpolation approach is so accurate in the case of u that the two curves are difficult to distinguish (Fig. 3(a)). The approach is less accurate for w, with TRACEO exhibiting some overshooting of the analytic solution (Fig. 3(b)), but still reproducing the interference pattern in both phase and amplitude along range.
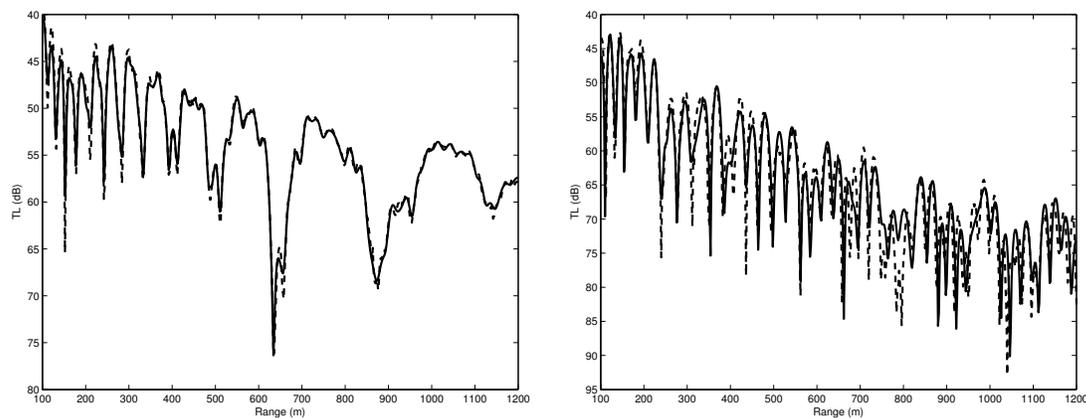

Figure 3: Particle velocity calculations for the Pekeris waveguide: u (left); w (right). In both cases the solid curve represents the analytic solution, while the dashed curve represents TRACEO's prediction.

4 SIMULATIONS

The performance of geoacoustic estimation using acoustic pressure or particle velocity components is discussed in this section through simulations of the Makai waveguide [8]. The discussion is divided in three parts, namely:

- TRACEO predictions will adress the performance of geoacoustic estimation when the Bartlett estimator is calculated using either p, u or w; the similarities and differences between the estimators will be outlined.

---

[1] http://www.siplab.fct.ualg.pt.

- TRACEO predictions for the best estimator will be validated through comparisons with the predictions provided by other models.

- TRACEO geoacoustic estimation using Δp will be compared with the estimation obtained with model predictions of w.

4.1 ESTIMATION USING P, V AND W

The geoacoustic estimation performed with TRACEO considers an idealized Makai waveguide, in which the true value of sediment compressional speed corresponds to 1570 m/s; during the experiment it was used a VSA with 4 hydrophones between depths 79.6 to 79.9 m, and signals were transmitted to a range of 1830 m. The Bartlett estimator was calculated at 13078 Hz in the interval from 1500 m/s to 1800 m/s using either p, u or w; the three estimators are shown in Fig.4. The figure
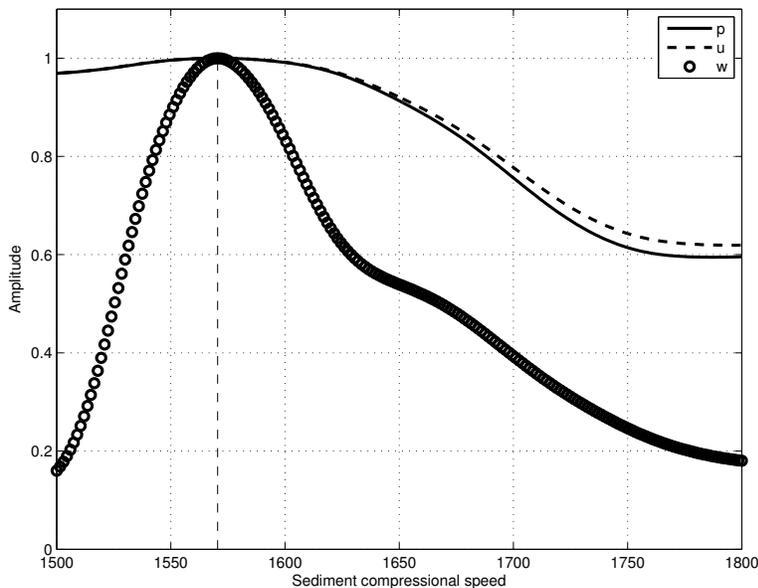

Figure 4: Bartlett estimators of compressional sound speed using acoustic pressure p, horizontal component of particle velocity u and vertical component of particle velocity w, calculated with TRACEO. The true value of compressional speed is indicated by the vertical dashed line.

reveals significant differences between the estimators using p or u, and the estimator using w; in fact, the first two estimators practically coincide, and exhibit a weak variation over the interval of considered compressional speeds; on the other side the estimator using w is significantly narrower over the same interval. Therefore, the results clearly indicate a clear advantage for geoacoustic estimation of using w over the use of either p or u.

4.2 ESTIMATION USING W WITH DIFFERENT MODELS

To further validate the geoacoustic estimation based on w from the previous section a new set of calculations was considered using three more acoustic models, namely KRAKEN (a normal mode model [2]), Bellhop (a Gaussian beam ray tracing model [4]) and MMPE (a parabolic equation model [6]). However, running KRAKEN and MMPE at 13078 Hz required such a fine discretization in depth and range which implied extremely long calculations, besides occupying significant disk space. To deal with both issues (and since the main purpose of the simulation is to validate geoacoustic estimation using w) it was decided to calculate the Bartlett estimator at 500 Hz for an idealized array with 6 hydrophones, between depths 75 to 80 m. The corresponding curves are shown in Fig.5; although the curves do not exhibit the same behaviour the general trend is very similar, with a narrow peak

around the true value of compressional sound speed. Remarkably, there is an excellent agreement between TRACEO and KRAKEN predictions. Such results confirm not only the advantage of relying on w for geoacoustic estimation, but also the validity of the interpolation approach for the calculation of particle velocity components.
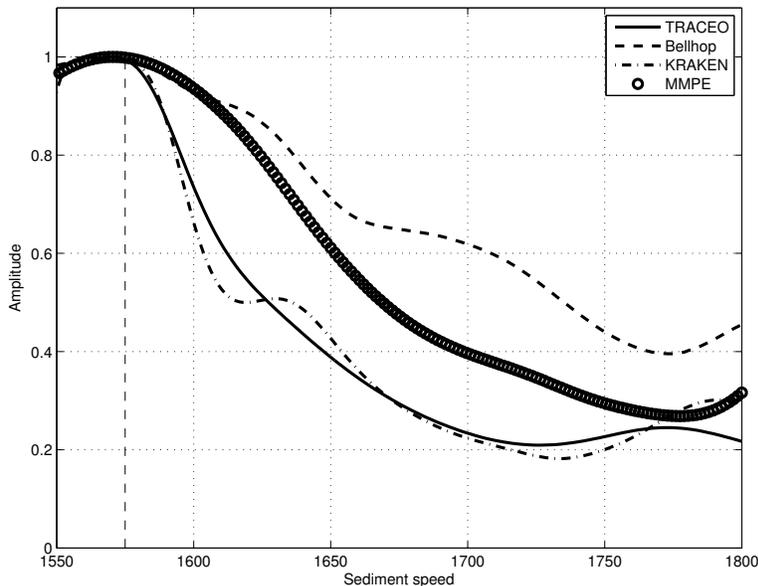

Figure 5: Bartlett estimators of compressional sound speed using w, calculated with TRACEO, Bellhop, KRAKEN and MMPE. The true value of compressional speed is indicated by the vertical dashed line.

4.3 ESTIMATION USING $\triangle P$ INSTEAD OF W

Following the results from the previous section the Makai waveguide was again considered as described in section 4.1, but with an hypothetical array of five standard hydrophones, located between depths 79.55 to 79.95 m. Acoustic pressure for such array was calculated again with TRACEO, and the "true" data was calculated as consecutive differences of acoustic pressure (2nd hyd minus 1st hyd, 3rd hyd minus 2nd. hyd, and so on); thus, the covariance matrix was calculated using such true data. Further, when calculating the Bartlett estimator, TRACEO predicted the values of w for an array of four hydrophones between depths 79.6 to 79.9 m. The results of geoacoustic estimation at 13078 Hz using both w and Δp are shown in Fig.6, which shows that the two curves coincide almost perfectly. However, data for the second curve would require an array of standard hydrophones, while the data for the first curve would require a VSA.

5 CONCLUSIONS AND FUTURE WORK

The discussion presented here is extremely encouraging for the development of VSAs with pairs of standard hydrophones, which would measure not only acoustic pressure but also the vertical component of particle velocity. The applications for geoacoustic estimation at high frequencies were positively outlined, and ray tracing models (despite apparent shortcomings) were shown to perform quite efficiently and accurately for estimation. There are, however, important issues that remain to be considered such as, for instance, if the accuracy of estimation is going to hold over arbitrary distances. Additionally, the sensitivity of estimation to noise corruption and to the type of ocean bottom (which implies significant differences in the values of compressional sound speed) will require detailed discussion in the future.
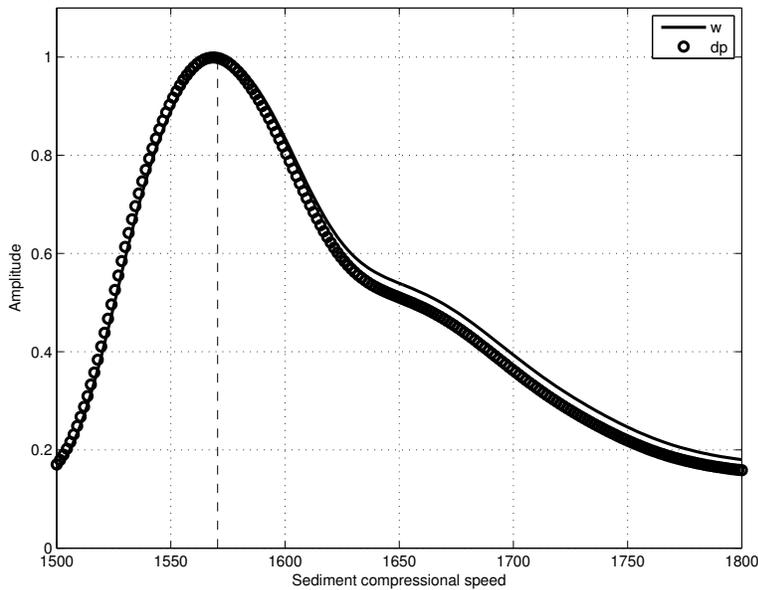
Figure 6: Bartlett estimators of compressional sound speed using w and Δp, calculated with TRACEO. The true value of compressional speed is indicated by the vertical dashed line.

ACKNOWLEDGEMENTS

REFERENCES

1. H. Schmidt. *SAFARI, Seismo–Acoustic Fast field Algorithm for Range – Independent enviroments. User's Guide*. Tech. report, SACLANT UNDERSEA RESEARCH CENTRE (SM-113), La Spezia, Italy, pp. 9-17, 1987.

2. M. Porter. *The KRAKEN normal mode program*. Tech. report, SACLANT UNDERSEA RESEARCH (memorandum), San Bartolomeo, Italy, page 8, 1991.

3. P. Felisberto, O. C. Rodríguez, P. Santos, and S. M. Jesus. On the usage of the particle velocity field for bottom characterization. In *Int. Conf. on Underwater Acoustic Measurements*, pp. 19–24, Kos, Greece, June 2011.

4. M. Porter and H. Bucker. Gaussian beam tracing for computing ocean acoustic fields. *J. Acoust. Soc. Am.*, 82(4): pp. 1349–1359, 1987.

5. K. Smith and F. Tappert. *UMPE: The University of Miami Parabolic Equation Model*. Tech. report, University of Miami (MPL Technical Memorandum 432), Miami, USA, pp. 45-48, 1994.

6. K. Smith. Convergence, stability, and variability of shallow water acoustic predictions using a split-step Fourier parabolic equation model. *J. Acoust. Soc. Am.*, 9(1): pp. 243–285, 2001.

7. P. Santos, P. Felisberto, O. C. Rodríguez, and S. M. Jesus. Geoacoustic Matched-field Inversion using a Vector Sensor Array. In *Conf. on Underwater Acoustic Measurements*, pp. 29–34, Nafplion, Greece, 21-26 June 2009.

8. P. Santos, O. C. Rodríguez, P. Felisberto, and S. M. Jesus. Seabed geoacoustic characterization with a vector sensor array. *J. Acoust. Soc. Am*, 5(128): pp. 2652–2663, November 2010.

9. P. Santos, P. Felisberto, O. C. Rodríguez, J. J. ao, and S. M. Jesus. Geometric and Seabed parameter estimation using a Vector Sensor Array - Experimental results from Makai experiment 2005. In *OCEANS2011*, pp. 1–10, Santander, Spain, June 2011.

10. F. Press and M. Ewing. Propagation of explosive sound in a liquid layer overlying a semi-infinite elastic solid. *Geophysics*, 15(3): pp. 426–446, 1950.